Research Article Vol. 60, No. 35 / 10 December 2021 / Applied Optics 10825

applied optics

Polarization-independent differential interference contrast and off-axis holography combined module

MATAN DUDAIE, SHIRA SHINAR, AND NATAN T. SHAKED*

Department of Biomedical Engineering, Faculty of Engineering, Tel Aviv University, Ramat Aviv, 69978 Tel Aviv, Israel
**Corresponding author: nshaked@tau.ac.il*

Received 31 August 2021; revised 3 November 2021; accepted 3 November 2021; posted 4 November 2021; published 3 December 2021

We present an external portable module for transforming bright-field microscopy to differential interference contrast (DIC) microscopy and digital holographic microscopy together. The module is composed of simple optical elements, positioned between the microscope output plane and the digital camera plane; thus, it can be integrated externally with existing microscopes. The proposed module enables polarization DIC imaging, without special polarization elements, under either white-light or coherent illumination, providing label-free imaging of biological samples, as recorded directly by the digital camera. In addition, by rotating one element inside the module, an off-axis hologram is created on the camera under coherent illumination, thus providing the possibility for reconstruction of the quantitative phase profile of the same sample. The method is demonstrated for imaging silica microspheres and biological cells.

https://doi.org/10.1364/AO.442065

1. INTRODUCTION

Differential interference contrast (DIC) microscopy is widely used for label-free imaging of transparent or semi-transparent biological samples [1]. Traditionally, DIC uses white-light illumination and polarization optics in the beam path, including two Wollaston or Nomarski prisms and two polarizers. These elements first split the illumination beam into two sheared beams passing through the sample with a small shear (~200 nm), where each beam has an orthogonal polarization in respect to the other beam and collects a slightly different optical path delay (OPD) of the sample. Then, the two 45° polarization projections of the beams are superimposed on the camera, resulting in qualitative label-free images with increased imaging contrast, resulted from the OPD gradient in the shear direction [2]. This conventional DIC method has an inherent disability to handle polarizing and birefringent samples. To overcome difficulties with birefringent samples, such as imaging cells on plastic substrates, PlasDIC was developed. It uses only one polarizer and one Wollaston prism after the sample, where two sheared beams interfere on the camera, and a DIC image is created [3]. Although PlasDIC can image samples in plastic dishes, it is still unsuitable for polarized illumination.

Integrating an external interferometer to a bright-field microscope can generate polarization-insensitive DIC microscopy, which uses no polarizing elements and thus is suitable for imaging on birefringent substrates as well as under polarized illumination, as previously proposed by us [4]. Chatterjee and Kumar suggested an unpolarized white-light DIC technique based on a Sagnac interferometer [5]. McIntyre *et al*. [6] proposed an external DIC system using a spatial light modulator. We also proposed an external DIC based on a Michelson interferometer illuminated by coherent light, and used it to characterize silicon wafer defects [7].

It has been previously shown that two or more DIC images with different shearing directions can be acquired and processed digitally to OPD image [8–14]. However, the fact that several camera exposures are required per each sample instance makes the method less attractive for highly dynamic processes. It is also possible to acquire two DIC images with orthogonal shears in a single exposure. However, in both cases, these images are processed to the OPD with a numerical reconstruction process, such as spiral phase integration, which is computationally heavy and prone to numerical errors [15,16].

Alternatively, the quantitative OPD of the sample can be obtained using a single off-axis hologram. Here, a coherent illumination source is used, and off-axis interference of the sample beam and a clear reference beam is recorded by the camera. Then, the complex wavefront of the sample can be digitally reconstructed, containing the OPD profile of the sample from a single camera shot [17,18]. Instead of splitting the beam to sample and reference beams at the exit of the illumination source, flipping interferometry (FI) allows obtaining the reference beam by using half of the sample beam, assuming that there are no sample details there, and flipping it on itself by using a two-mirror retroreflector [19].

The OPD image can be used to calculate a DIC image digitally, by subtracting the OPD from itself with a small shift [20–22]. However, in contrast to the first mode of the proposed module, the synthetic DIC image does not appear on the camera or in the eyepieces directly, since the OPD must be digitally reconstructed first. In addition, the resulting DIC image contains a higher spatial noise originated from the speckle noise in the original OPD image.

Many external add-on modules for existing optical microscope implementing DIC or holography have been proposed [16,23–26]. However, usually, DIC microscopy and off-axis holography are two distinct methods.

In this paper, we present an external module combining DIC and FI setups. The module is positioned between the microscope output and a digital camera. It can create on the camera a polarization-insensitive DIC image, with fully adjustable shear offset and direction, integrated with an off-axis image hologram based on FI, using the exact same optical elements. Thus, for the first time, the operator can use a single external optical module to obtain both optical DIC and OPD images for the same field of view of the sample. The switching between the modes is done by rotating a retroreflector inside the module and using either the microscope's white-light source for the DIC mode or a coherent light source for the FI mode.

2. COMBINED DIC-FI SETUP

The proposed DIC-FI module is depicted in Fig. 1. The module is connected to the microscope output plane (MOP) of an inverted microscope, as illustrated in Fig. 1(a). Figure 1(b) shows a photo of the proposed module. The DIC mode of the module is shown in Fig. 1(c). A Michelson interferometer with a 4f achromatic lens system (L1 and L2) collects the bright-field image from the microscope. After beam splitter BS, two mirrors are placed at the Fourier planes of lens L1. At one of the Fourier planes, a flat mirror is positioned, and the beam is reflected back through the exit lens L2 onto the camera. At the other Fourier plane after the beam splitter, a hollow retroreflector RR mirror is placed in almost 90 deg so that one of its faces is used as a simple mirror, and no secondary reflection occurs. This mirror is slightly tilted, returning a small constant phase shift to the Fourier plane so that after lens L2, a shear is created on the image plane on the camera. The sheared sample image is superimposed with the first sample image on the camera. One of the mirrors is positioned in a path-length difference of a multiple of a quarter of a wavelength to produce a deconstructive interference, thus generating the DIC image.

To swap the module to the FI mode shown in Fig. 1(d), the retroreflector is rotated, and the coherent source is activated. Here, the retroreflector flips the image, so on the camera plane, we get an interference between two halves of the field of view, which is suitable for sparse samples, or non-sparse samples located only in half of the field of view, such as cells flowing in a microfluidic channel [19]. The retroreflector shifts the center of the Fourier plane by its transverse location, so that an off-axis angle is obtained for the reflected beam projected onto the camera.

In typical DIC, the shear between the beams is approximately 200 nm on the sample plane. However, in the DIC mode of the module, splitting and combining the beam are accomplished externally to the imaging system, so the required shear distance after the total magnification is set to approximately one camera pixel. Otherwise, the image could look smeared, doubled, or blurry.

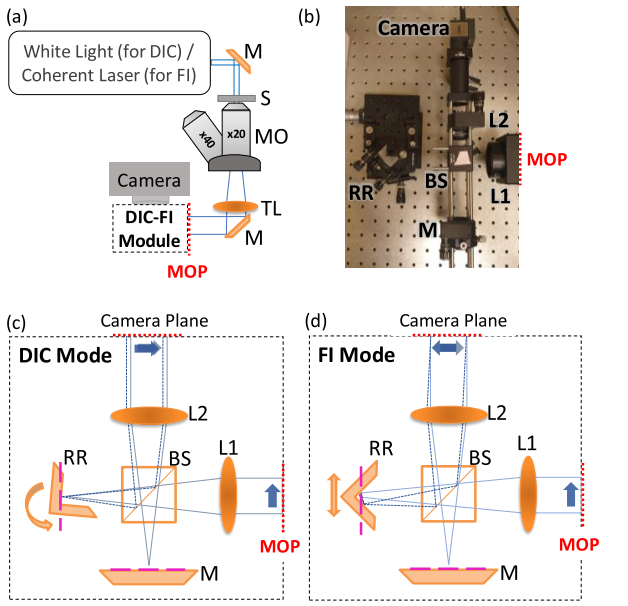

Fig. 1. Proposed optical setup. (a) DIC-FI module, connected at the exit of an inverted microscope illuminated by a white-light source and a coherent source. (b) Photo of the module from top view. (c) DIC mode of the module, where a DIC image is created on the camera. (d) FI mode of the module, where an off-axis hologram is created on the camera. M, mirror; MO, microscope objective; TL, tube lens; L1, L2, lenses in 4f configuration; BS, beam splitter; RR, hollow retroreflector; MOP, microscope output plane.

For the experimental setup, we used a commercial inverted microscope (Zeiss AxioObserver D1) and connected the custom-built DIC-FI module to its camera port. The microscope was also equipped with PlasDIC, used for validation of the DIC-FI module results. In the module, we used lenses L1 and L2 with $f = 150$ mm each, HRS1015-P01 hollow retroreflector (Thorlabs), and UI-3060CP Rev. 2 camera (IDS) with pixel size of 5.8 μm. For DIC, we used the LED lamp provided with the microscope. For FI, we used a coherent 532 nm laser (LRS-PFM-00050, LaserGlow). The diffraction-limited spot size was 875 nm or 1330 nm, depending on the microscope objective used. The spatial phase sensitivity was 0.18 ± 33 mrad/s. The depth of focus was 137 μm. For OPD reconstruction, we used the off-axis holographic Fourier-based algorithm, followed by two-dimensional phase unwrapping [27].

In DIC mode, to align the fixed mirror at the Fourier plane, we first used the coherent light source of the FI mode to approximately position the retroreflector mirror by finding the focused beam location using the on-axis interference pattern. Subsequently, we switched to the white-light source and slowly moved the retroreflector to find the exact position for the deconstructive interference. The offset shear and direction can be controlled by slightly tilting the retroreflector. The shear was set to give the best DIC image and was measured to be about one pixel. This alignment can be done only once. To swap to FI

mode, we rotated the retroreflector and switched to coherent light.

3. EXPERIMENTAL RESULTS

We first imaged 10 μm silica beads (904368, Sigma-Aldrich) immersed in mineral oil (Sigma-Aldrich) using a 40×, 0.6 NA microscope objective. Figure 2(a) shows the bright-field image of the beads, which does not have a DIC effect, and Fig. 2(b) shows the coinciding PlasDIC image, which has a DIC effect. Figures 2(c) and 2(d) present DIC images obtained by our DIC-FI module, while selecting horizontal and vertical shears, respectively. The bottom bead gray-level cross sections at its center along the shear directions marked with arrows, are shown under each image.

Figure 2(e) presents the reconstructed OPD [18] from the hologram obtained by the module in the FI mode (off-axis hologram shown in the yellow box), with the central cross-section profile shown at the bottom. The refractive index of the silica beads is 1.46, and of mineral oil is 1.48, resulting in 200 nm as the the maximum OPD value of the bead . Figure 2(f) shows a synthetic DIC image obtained by subtracting the OPD of Fig. 2(e) from a slightly shifted version of itself, demonstrating that although we obtain high DIC contrast, higher spatial noise is present in the synthetic DIC image in comparison to the optical DIC image.

To assess the DIC-FI polarization-insensitive imaging abilities, we imaged a USAF resolution phase target. Figure 3(a) shows the bright-field imaged target (group 4, element 4) under 20× magnification (0.4 NA) under linearly polarized white light. When imaging it with PlasDIC, the sample is

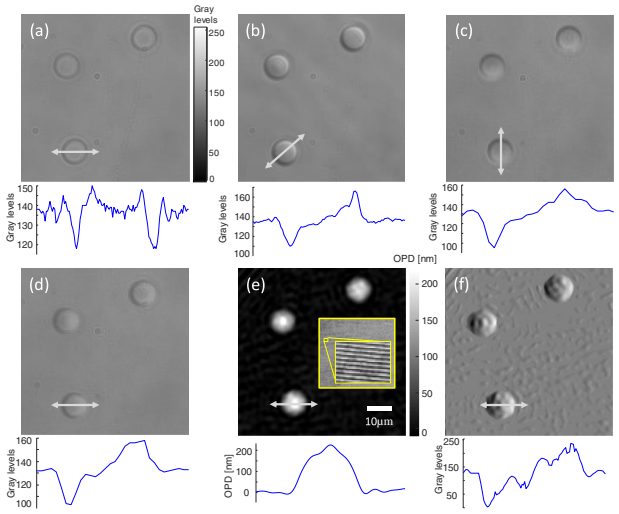

Fig. 2. Imaging 10 μm silica beads. (a) Bright-field image, where the beads are mostly transparent, and its cross section along the arrow. (b) PlasDIC image, and its cross section along the arrow, where DIC effect is seen. (c), (d) DIC images obtained with the DIC-FI module in DIC mode with different shear directions, and their cross sections along the arrows. (e) OPD profile digitally reconstructed from the off-axis hologram, shown in the yellow box, as obtained by the DIC-FI module in FI mode. The OPD cross section along the center of the bottom bead is shown at the bottom. (f) Synthetic DIC image obtained from the OPD image in (e). Arrow orientations in (b)–(d) and (f) indicate the shear directions in the DIC images.

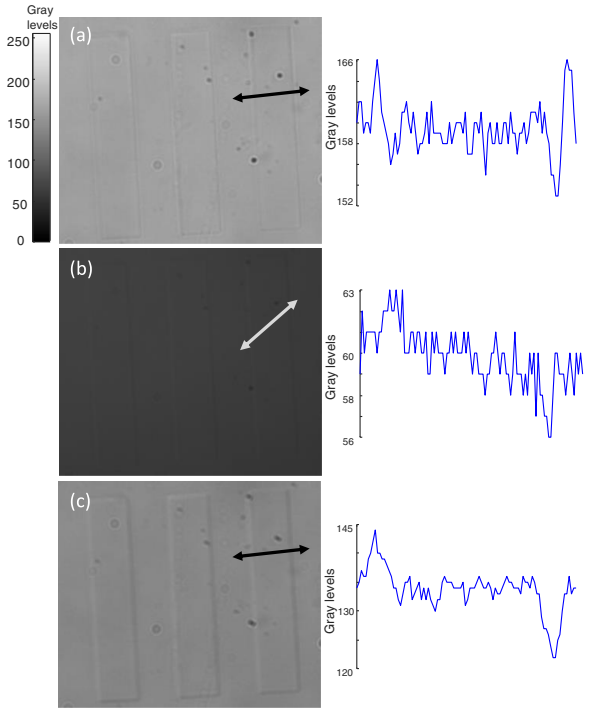

Fig. 3. DIC imaging comparison under polarized white light of a USAF resolution phase target. (a) Bright-field image. (b) PlasDIC image. (c) DIC image obtained by the proposed DIC-FI module. Cross-section profiles along arrows are shown on the right. Arrow orientations in (b) and (c) indicate the shear directions.

almost invisible [Fig. 3(b)], even with a long exposure time (>350 msec) and maximum brightness of the microscope, due to using polarized illumination, which was almost orthogonal to the PlasDIC polarizer. In contrast, when imaging the sample under polarized light with the DIC-FI module in DIC mode, the DIC effect is seen clearly [Figs. 3(c)]. The coinciding cross sections at the center of the right bar are shown on the right.

Note that the USAF test target lines are not orthogonal to the shear direction in Fig. 3(b), resulting in a poor DIC effect in the PlasDIC image. In contrast, with the DIC-FI, we can control the shear direction to match the sample orientation.

Next, we imaged MCF-7 breast cancer cells. The cells were incubated for three days to attach and spread on a microscope slide, and then fixated using 4% paraformaldehyde. Figure 4(a) shows selected cells under bright-field imaging. Figure 4(b) shows the same cells imaged with the DIC-FI module in DIC mode. The contrast of the DIC image can further increase when using the coherent light source, as shown in Fig. 4(c). Figure 4(d) shows the reconstructed OPD profile obtained using the FI mode of the module. As shown in Fig. 4, the cells are hardly visible in the bright-field image [Fig. 4(a)] and become detectable using the module under either white light or coherent light [Figs. 4(b) and 4(c), respectively], and the quantitative OPD profile of the same cells can be easily obtained with the same module [Fig. 4(d)].

To examine the suggested system polarization-independence property, we imaged a drop of a microscope immersion oil (Olympus) on a plastic petri dish, exhibiting birefringent properties. Figure 5(a) shows an image of the oil drop under 10×

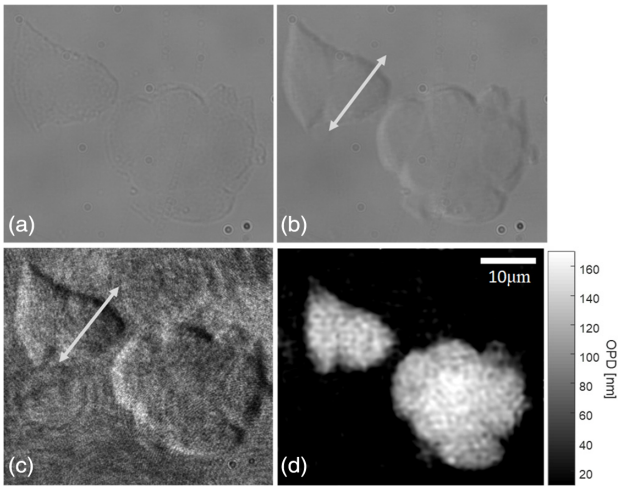

Fig. 4. Imaging MCF7 breast cancer cells. (a) Bright-field image, where the cells are hardly visible. (b) DIC image obtained by the DIC-FI module under white-light illumination. (c) DIC image obtained by the DIC-FI module under coherent illumination (d) Reconstructed OPD profile as obtained from the off-axis hologram recorded by the DIC-FI module in FI mode.

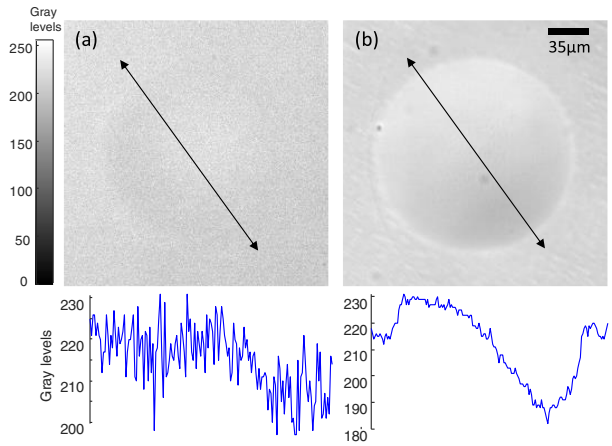

Fig. 5. DIC imaging comparison of a microscope immersion oil drop on a plastic dish (birefringent), using: (a) conventional DIC microscopy, containing two Nomarski prisms, and (b) the proposed DIC-FI module. Cross sections along the marked arrows are presented under each image.

magnification with a conventional two-Nomarski-prisms DIC microscope (IX83, Olympus), where the oil drop is almost invisible. Figure 5(b) shows the same drop using the suggested DIC-FI system, demonstrating a visible DIC effect with higher contrast.

4. DISCUSSION

Because the PlasDIC microscope uses polarization and a slit diaphragm, the field aperture and field diaphragm are fully open to receive bright and clear images in long exposure times (~300 msec). For the DIC-FI, the white-light source is bright enough even in lower settings; therefore, we can decrease the field aperture substantially, thus increasing the spatial coherence and producing higher contrast interference images. In spite of decreasing the amount of light, we did not lose any brightness and could image in exposure times of 25 msec or less, which is suitable for dynamic samples.

Swapping between the module DIC and FI modes is easy to perform. This is done by rotating the retroreflector stage by not more than 10°, turning on the laser, and turning off the white-light illumination. Once the system is aligned and the destructive coherence is achieved, swapping between the modes can be performed repeatedly within only a few seconds if done manually or even faster if automated. We used manual instruments to hold and align the mirrors. By using motorized or piezoelectric elements, higher contrast images can possibly be obtained.

Since the module is external to the microscope, one can choose the optical elements to best fit the module performance. Achromatic lenses are used to avoid chromatic aberrations. Aspheric lenses are used to avoid field-curvature aberrations. The camera pixel size is chosen so that each diffraction-limited spot, as defined by the optical system numerical aperture and the central wavelength, is imaged on approximately eight pixels on the camera, which is a tighter condition than the one required for the DIC mode and therefore appropriate for this mode as well. The hologram fringe-frequency cycle is chosen to occupy approximately three pixels on the camera.

Since the FI mode and the resulting quantitative phase image interpretation are limited to thin samples, such as a single monolayer of cells, the DIC mode is also generally applicable to these thin samples. Although a digital holography-based DIC image with controllable shearing direction (as well as other digital effects such as a dark-field image) can be generated from the OPD image [18], coherent noise does not allow holography-based DIC to yield a clear image as in optical DIC. This is relevant for thin objects or fine details, which might be missed in holography-based DIC. The fact that the proposed optical DIC does not require processing (the image appears directly on the camera or in the eyepieces) allows faster imaging since no digital phase extraction is needed. Also, many biologists prefer to view the DIC image directly in the eyepieces, since a larger field of view is obtained. All of these motivate the usefulness of the proposed combined DIC-FI module.

5. CONCLUSION

To summarize, we presented the DIC-FI module, a polarization-insensitive combined setup for qualitative and quantitative label-free imaging. This system allows a bright-field light microscope to turn into a DIC microscope without any digital processing. With the addition of coherent light, it can serve as both a high-contrast DIC system and an off-axis holographic system, where the switch between the modes is done by simply tilting the retroreflector inside the module. The DIC images can be obtained with the maximum brightness of the microscope. With this module, we can also control the shearing offset length and direction and have the ability to image directional samples without the need to rotate the sample itself. The FI mode enables direct quantitative phase imaging of the exact same sample area. Finally, note that this paper does not propose a multi-model system, being able to simultaneously acquire the same instance of the sample with two imaging modalities.

Instead, we propose a simple external module of two imaging modes, with the same optical elements: optical polarization-insensitive DIC without digital processing or quantitative phase imaging, with simple swapping between the modes. This module can be a useful tool for adjusting existing microscopes, which have neither DIC nor holography, to have these label-free imaging abilities for imaging transparent biological samples.

Acknowledgment. We thank Dr. Itay Barnea for the biological sample preparation.

Disclosures. The authors declare no conflicts of interest.

Data Availability. No data were generated or analyzed in the presented research.

REFERENCES

1. D. B. Murphy, *Fundamentals of Light Microscopy and Electronic Imaging* (Wiley-Liss, 2001).
2. J. Mertz, *Introduction to Optical Microscopy* (Cambridge University, 2019).
3. R. Danz, A. Vogelgsang, and R. Käthner, "PlasDIC—a useful modification of the differential interference contrast according to Smith/Nomarski in transmitted light arrangement," Photonik **1**, 42–45 (2004).
4. P. Girshovitz and N. T. Shaked, "Polarization-independent differential interference contrast optical arrangement," U.S. patent application 0259158A1 (2016).
5. S. Chatterjee and Y. P. Kumar, "Un-polarized light transmission DIC microscope," J. Opt. **45**, 297–301 (2016).
6. T. J. McIntyre, C. Maurer, S. Bernet, and M. Ritsch-Marte, "Differential interference contrast imaging using a spatial light modulator," Opt. Lett. **34**, 2988–2990 (2009).
7. A. Nativ, H. Feldman, and N. T. Shaked, "Wafer defect detection by a polarization-insensitive external differential interference contrast module," Appl. Opt. **57**, 3534–3538 (2018).
8. L. Xiomara and B. Rozo, *Phase estimation for Differential Interference Contrast Microscopy* (University Côte d'Azur, 2017).
9. C. Zhou, T. Huang, Z. Wang, S. Liu, L. Zhong, G. Pendrini, C. Yuan, and X. Lu, "Self-compensating quantitative differential interference contrast microscopy imaging system using liquid crystal shearing assembly," Opt. Laser Eng. **136**, 106325 (2021).
10. S. B. Mehta and C. J. R. Sheppard, "Partially coherent image formation in differential interference contrast (DIC) microscope," Opt. Express **16**, 19462–19479 (2008).
11. M. Shribak and S. Inoué, "Orientation-independent differential interference contrast microscopy," Appl. Opt. **45**, 460–469 (2006).
12. T. J. McIntyre, C. Maurer, S. Fassl, S. Khan, S. Bernet, and M. Ritsch-Marte, "Quantitative SLM-based differential interference contrast imaging," Opt. Express **18**, 14063–14078 (2010).
13. G. Vishnyakov, G. Levin, V. Minaev, M. Latushko, N. Nekrasov, and V. Pickalov, "Differential interference contrast tomography," Opt. Lett. **41**, 3037–3040 (2016).
14. S. V. King, A. Libertun, R. Piestun, C. J. Cogswell, and C. Preza, "Quantitative phase microscopy through differential interference imaging," J. Biomed. Opt. **13**, 024020 (2008).
15. D. Fu, S. Oh, W. Choi, T. Yamauchi, A. Dorn, Z. Yaqoob, R. R. Dasari, and M. S. Feld, "Quantitative DIC microscopy using an off-axis self-interference approach," Opt. Lett. **35**, 2370–2372 (2010).
16. P. Bon, G. Maucort, B. Wattellier, and S. Monneret, "Quadriwave lateral shearing interferometry for quantitative phase microscopy of living cells," Opt. Express **17**, 13080–13094 (2009).
17. N. T. Shaked, "Quantitative phase microscopy of biological samples using a portable interferometer," Opt. Lett. **37**, 2016–2018 (2012).
18. P. Girshovitz and N. T. Shaked, "Real-time quantitative phase reconstruction in off-axis digital holography using multiplexing," Opt. Lett. **39**, 2262–2265 (2014).
19. D. Roitshtain, N. A. Turko, B. Javidi, and N. T. Shaked, "Flipping interferometry and its application for quantitative phase microscopy in a micro-channel," Opt. Lett. **41**, 2354–2357 (2016).
20. L. Miccio, A. Finizio, R. Puglisi, D. Balduzzi, A. Galli, and P. Ferraro, "Dynamic DIC by digital holography microscopy for enhancing phase-contrast visualization," Biomed. Opt. Express **2**, 331–344 (2011).
21. L. Miccio, A. Finizio, P. Memmolo, M. Paturzo, F. Merola, G. Coppola, G. Di Caprio, M. Gioffrè, R. Puglisi, D. Balduzzi, A. Galli, and P. Ferraro, "Detection and visualization improvement of spermatozoa cells by digital holography," Proc. SPIE **8089**, 80890C (2011).
22. X. Yu, M. Cross, C. Liu, D. C. Clark, D. T. Haynie, and M. K. Kim, "Measurement of the traction force of biological cells by digital holography," Biomed. Opt. Express **3**, 153–159 (2012).
23. T. H. Nguyen, M. E. Kandel, M. Rubessa, M. B. Wheeler, and G. Popescu, "Gradient light interference microscopy for 3D imaging of unlabeled specimens," Nat. Commun. **8**, 210 (2017).
24. P. Girshovitz and N. T. Shaked, "Doubling the field of view in off-axis low-coherence interferometric imaging," Light Sci. Appl. **3**, e151 (2014).
25. N. A. Turko and N. T. Shaked, "Simultaneous two-wavelength phase unwrapping using an external module for multiplexing off-axis holography," Opt. Lett. **42**, 73–76 (2017).
26. J. A. Picazo-Bueno, M. Trusiak, and V. Micó, "Single-shot slightly off-axis digital holographic microscopy with add-on module based on beamsplitter cube," Opt. Express **27**, 5655–5669 (2019).
27. N. T. Shaked, Y. Zhu, M. T. Rinehart, and A. Wax, "Two-step-only phase-shifting interferometry with optimized detector bandwidth for microscopy of live cells," Opt. Express **17**, 15585–15591 (2009).